



Cite this: *Green Chem.*, 2025, **27**, 4341

# Sustainable and biobased self-blown polycarbonate foams: from synthesis to application†

Tansu Abbasoglu,<sup>a</sup> Xavier Lopez de Pariza,<sup>a</sup> Gabriel Perli,<sup>a</sup> Danila Merino,<sup>a,b</sup> Phœbé Caillard-Humeau,<sup>c,d</sup> Antoine Duval,<sup>c,d</sup> Luc Avérous,<sup>c</sup> Lourdes Irusta,<sup>a</sup> Alba González<sup>a</sup> and Haritz Sardon<sup>a</sup> <sup>\*a</sup>

Escalating environmental concerns driven by the continuous demand for fossil-based materials have sparked growing interest in designing biobased polymeric materials for high-added-value applications. A novel series of self-blowing polycarbonate foams derived from various biobased polyols (e.g. cashew nut-shell liquid, vegetable oil, and lignocellulose) is reported by leveraging thiol-triggered carbon dioxide release in a formulation composed of a thiol and 5- and 6-membered cyclic carbonates. The polyol architecture enabled a tunable open-cell morphology and properties, achieving up to 41 wt% biobased content, marking the first incorporation of biobased monomers in this type of foam. In this context, cashew nutshell-based foam featured good cyclic endurance at 70% compression and a high-water uptake capacity of 8 g g<sup>-1</sup>. As a forward-looking solution to address environmental challenges, this foam effectively supports the germination of different types of vegetable seeds (e.g. bok choy (*Brassica rapa chinensis*), lettuce (*Lactuca sativa*), and radish (*Raphanus sativus*)) in soilless environments, and its hydrolytic stability ensures reusability for subsequent seedling growth. This study lays the foundation for designing future environmentally friendly and renewable polymeric foams that are potentially recyclable with sustainable applications, e.g., in hydroponics.

Received 20th December 2024,  
Accepted 7th March 2025

DOI: 10.1039/d4gc06429a

[rsc.li/greenchem](https://rsc.li/greenchem)

## Green foundation

1. In the quest to circumvent the need for toxic isocyanates (common in PU production) and external blowing agents (for foam expansion), we rely on a versatile green foaming strategy that mimics the conventional polyurethane self-foaming to design foam materials based on recyclable polycarbonates. To increase the biobased content, we incorporate renewable polyols derived from biomass sources (vegetable oils, cashew nutshell liquid, and lignin) into the formulation. We address the challenge of recycling out-of-service foams by upcycling thermoset polycarbonate foams into second-life materials.
2. We describe the first study on biobased self-blowing polycarbonate foams, achieving diverse open-cell morphologies and properties with a biobased content of up to 41 wt% from a single formulation using a range of different biobased polyols. This study draws a full picture of sustainable materials design: from synthesis following green chemistry principles (avoidance of toxic precursors, lower energy consumption through a single-step mild reaction, the use of renewable raw materials) to application as a green and recyclable substrate in soilless farming, addressing food production and environmental sustainability challenges.
3. Further research could focus on increasing the biobased content of polycarbonate foams by exploring novel biobased poly(6-membered cyclic carbonates). More interesting, perhaps, is to valorise recycled polyols from biomass waste (lignocellulosic residues, food industry by-products, or agricultural leftovers) for foam production. To fully understand the benefits of biobased polycarbonate foams, their biodegradation (soil and enzymatic) should be investigated. Cashew nutshell liquid can impart additional functions, such as antimicrobial properties, which could provide protection against plant pathogens and warrant further investigation.

<sup>a</sup>POLYMAT, Department of Advanced Polymers and Materials: Physics, Chemistry and Technology, University of the Basque Country UPV/EHU, Joxe Mari Korta Center, Avda. Tolosa 72, 20018 Donostia, San Sebastián, Spain.

E-mail: [haritz.sardon@ehu.eus](mailto:haritz.sardon@ehu.eus)

<sup>b</sup>Ikerbasque, Basque Foundation for Science, 48009 Bilbao, Spain

<sup>c</sup>BioTeam/ICPEES-ECPM, UMR CNRS 7515, Université de Strasbourg, 25 rue Becquerel, 67087, Strasbourg, Cedex 2 France

<sup>d</sup>Soprema, 15 rue de Saint-Nazaire, 67100 Strasbourg, France

† Electronic supplementary information (ESI) available. See DOI: <https://doi.org/10.1039/d4gc06429a>

## 1 Introduction

From a materials perspective, cellular polymers (polymeric foams) have a unique combination of properties, such as a very low density, high energy absorbing capacity in compression, low thermal conductivity, or filtration ability that are derived from their porous morphology.<sup>1,2</sup> These porous polymers have thus found a wide variety of industrial applications, from thermal or noise insulation and impact absorption/cushioning



(for example, mattresses, packaging, and personal protection gear) to water treatment.<sup>3–5</sup> Among the plethora of largely available polymers, polyurethane (PU) is predominantly used for foam production (about 2/3), with a yearly worldwide production of 12 million tons.<sup>6</sup> Yet, PU materials are mostly derived from fossil resources, which is not sustainable.<sup>7</sup> Conveniently, in the presence of water, the foaming of PUs involves the release of CO<sub>2</sub> from the partial hydrolysis of isocyanates, which simultaneously polymerize with polyols. This dual function of isocyanates enables self-blowing (or self-foaming) and cross-linking, making them straightforward candidates for polymeric foam production. However, increasingly stringent European regulations are imposing stricter limits on the use and exposure to isocyanates to protect both human health and the environment from their toxic effects.<sup>8</sup> From a sustainability perspective, it is therefore crucial for constructing greener biobased foams, to consider isocyanate-free processes, akin to the PU self-blowing methods.

Over the last decade, much effort has been devoted toward the development of polyhydroxyurethanes (PHUs) obtained from the polyaddition of polyamines to poly(5-membered cyclic carbonate)s to design isocyanate-free PU foams. Since in the past it was believed that such systems do not possess self-blowing ability, external gases were used to promote their foaming.<sup>9–15</sup> Recently, the group of Detrembleur reported the ability of 5-membered cyclic carbonates (5-CCs) to release CO<sub>2</sub> in the presence of thiols and water.<sup>16–18</sup> This approach, besides being more sustainable without the use of toxic isocyanates, provides new opportunities in the field of cellular materials.

Aliphatic polycarbonates (PC)s are drawing renewed attention for creating sustainable polymer materials because they can be easily bio-derived and degraded into non-toxic products, such as small alcohols and carbon dioxide.<sup>19–22</sup> Until now, much research has been focused on developing aliphatic PC-based materials for diverse fields of applications, such as drug delivery, tissue regeneration as 3D printing scaffolds, batteries, and stimuli-responsive materials.<sup>22–24</sup> Despite such promise, PC foams are still typically made from aromatic thermoplastics like Lexan, which are externally blown using physical blowing agents (*e.g.*, N<sub>2</sub>, CO<sub>2</sub>, or *n*-pentane).<sup>25–29</sup> External blowing methods add cost and complexity to manufacturing, highlighting the need for a self-blowing process with PCs. Very recently, our group introduced for the first time CO<sub>2</sub> self-blown PC foams by incorporating thiols into a formulation of 5- and 6-membered cyclic carbonates (5-CC and 6-CC) and polyols.<sup>30</sup>

Besides higher degradability, another important feature of self-blown PC foams in comparison to self-blown PHU foams is that they are primarily prepared from polyols instead of polyamines. While recently bio-waste-based composite self-blown PHU foams have been developed to increase the material's biobased content,<sup>31</sup> the industrial availability of biobased amines is still limited compared to renewable polyols which results in a significant drawback for the industrial development of this kind of material.<sup>32,33</sup> A large variety of sustainable polyols

from biomass resources (vegetable oils,<sup>34</sup> sugars,<sup>35</sup> or lignocellulosic biomass<sup>36</sup>) are commercially available and primarily incorporated into traditional PU formulations. Besides, different sustainable polyols can also be largely available from chemical recycling processes.<sup>34</sup> Because such diverse origins offer the potential for structural diversification, a wide toolbox is accessible to tune the properties of the final material.<sup>37,38</sup>

Building on our previous work,<sup>30</sup> we herein replace a fossil-based polyol (polycaprolactone triol) with biobased polyols in self-blowing PC formulations to reduce the use of nonrenewable resources, resulting in a range of open-cell foam morphologies with a high biobased content, hydrophilic behavior, and hydrolytic stability.

Considering these different behaviors, soilless food production can be targeted as a proof-of-concept application while also demonstrating the biocompatibility of foams through a simple germination bioassay.<sup>39</sup> Some polymers, including PU and phenolic resins, have already been used for fabricating growing substrates due to their beneficial properties intrinsic to cellular plastics, such as tunable porous structures, shape retention, stability, and water- and air-holding abilities, which make polymer foams particularly suitable.<sup>40,41</sup> Therefore, in this work, we explore the potential of PC foams to germinate different types of vegetable seeds (bok choy (*Brassica rapa chinensis*), lettuce (*Lactuca sativa*), and radish (*Raphanus sativus*)). Biobased self-blown PC foams could thus overcome the challenges and hold promise as greener foams for new-generation applications.

## 2 Results and discussion

### 2.1 Foam formulations from various types of biobased polyols

We have previously shown that, thanks to the selective attack by the thiol nucleophile on 5-CC, it leads to the *in situ* formation of CO<sub>2</sub> and a reactive  $\beta$ -hydroxyl *S*-alkylated intermediate, while concurrently the cross-linked PC arises from the ring-opening polymerization of 6-CC by alcohols (Fig. 1a).<sup>30</sup> This process can be understood based on the orthogonal reactivity of thiols and alcohols with cyclic carbonates of 5 and 6 members. In this sense, first, we wanted to evaluate the versatility of this technology and its feasibility to implement with a series of biobased polyols of diverse chemical nature (*e.g.* phenolic and aliphatic) and functionality.

In this way, four different polyols from various botanical sources were used to develop polycarbonate foams. Their idealized chemical structures and respective biomass feedstocks are depicted in Fig. 1a. Full names are provided in Table S1 in the ESI.† We used aromatic polyols derived from cashew nutshell liquid (CNSL) using Cardolite's commercial technology<sup>42</sup> as well as from lignocellulose. Lignin, the most abundant source of renewable aromatics, provides promising opportunities for feasible modifications and tunable hydroxyl-functionalities.<sup>43</sup> The lignin-based polyol, namely Lignin-PEG, was synthesized



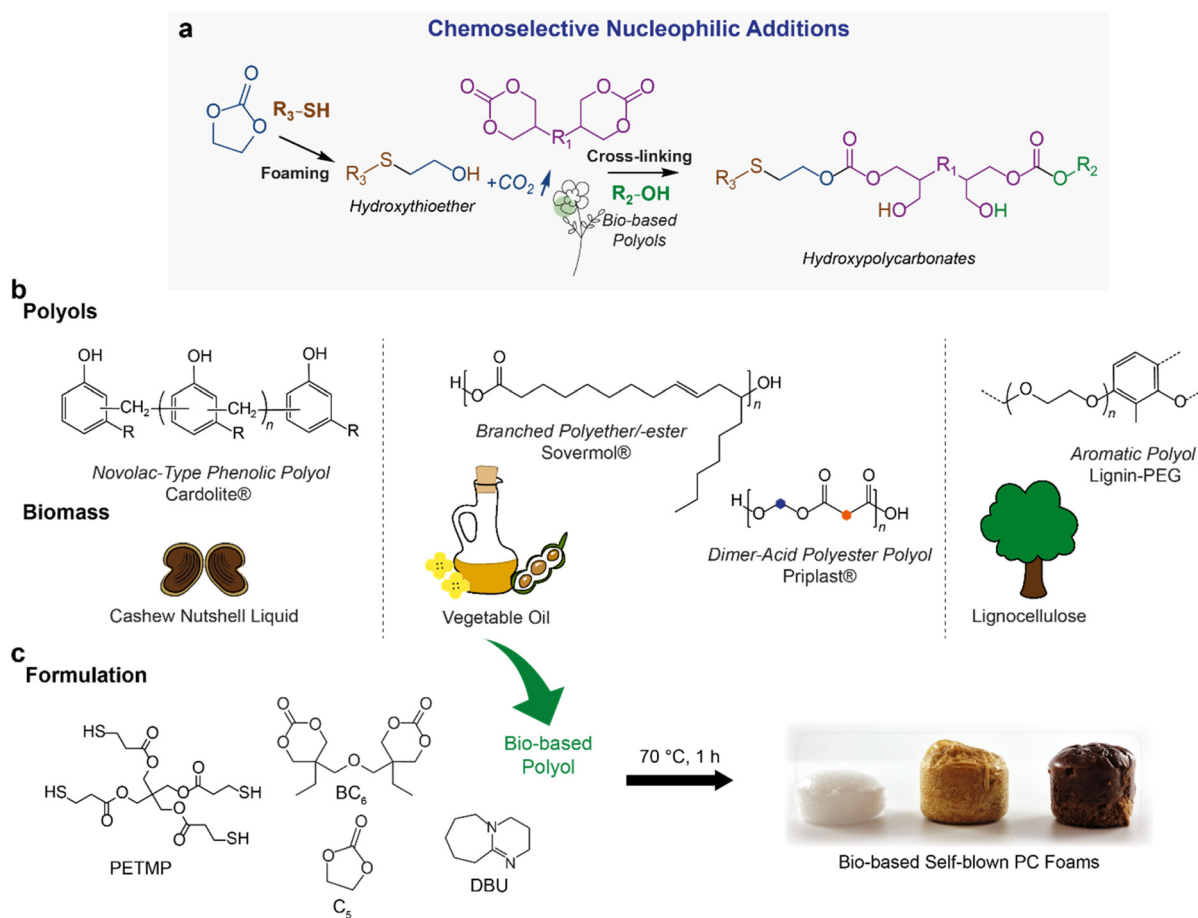


**Fig. 1** General strategy for self-blown PC foams. (a) Cascade ring-opening polymerization involving two chemoselective nucleophilic additions: 5-CC reacts with thiols while 6-CC reacts with alcohols. This results in foaming and the PC matrix formation, respectively. The self-blowing PC foaming method now incorporates biobased polyols. Simplified structures for clarity. (b) Biobased polyols and their corresponding biomass feedstocks with idealized structures.<sup>34,42–45</sup> Commercial names are indicated with the registered trademark symbol (®). (c) PC formulation consisting of BC<sub>6</sub>, C<sub>5</sub>, PETMP, and one of the biobased polyols shown in (b). The foaming process occurs in the presence of the base catalyst, DBU at 70 °C for 1 h. Formulation compositions of each polyol type are detailed in Table S1 (ESI).†

by modifying Kraft lignin with ethylene carbonate in polyethylene glycol (PEG), as schematically illustrated in Fig. S1 of the ESI.† Successful grafting of ethylene oxide groups onto the lignin core was confirmed by <sup>31</sup>P NMR (for full characterization, see the ESI†). Alternatively, vegetable oil-derived polyols include a branched polyether/-ester polyol under the trade name Sovermol<sup>44</sup> and a Priplast<sup>45</sup> dimer-acid-based difunctional polyester polyol.

For the fabrication of the PC foams, bis(6-membered cyclic carbonate) (di(trimethylolpropane) carbonate, BC<sub>6</sub>), a mono-functional 5-membered cyclic carbonate (ethylene carbonate, C<sub>5</sub>), and the tetrathiol (pentaerythritol tetrakis(3-mercaptopropionate), PETMP) with one type of biobased polyol were mixed in the presence of DBU as a catalyst for 1 h at 70 °C (Fig. 1b). We worked according to our previously reported optimal formulation<sup>30</sup> with a fixed BC<sub>6</sub>/C<sub>5</sub>/PETMP ratio of 1 : 1 : 0.25, with the cyclic carbonate functionality of BC<sub>6</sub> in excess of the moles of hydroxyl groups (2 : 1.5; thus, OH from the polyol/BC<sub>6</sub> = 1 : 0.5). Table S1 (ESI)† summarizes the molar equivalents of

each polyol relative to BC<sub>6</sub>, calculated from the known number of their hydroxyl groups. In addition, a surfactant (Tegomer E-Si 2330) was added at 10 wt% regarding the cyclic carbonates to produce uniform and stable bubbles and keep the gas inside the material during the process.<sup>18</sup> A series of foams with different types of renewable polyols and varying biobased contents (up to 41%) was successfully produced (Table 1). During the foaming and simultaneous crosslinking process, the storage modulus *G'* rapidly increases until becoming larger than the loss modulus *G''* by an order of magnitude (as attested by rheological measurements in Fig. S3†), indicating gelation. The gel time (determined when *G'* = *G''*) was achieved in all the cases within 4 minutes. The formation of the polycarbonate (PC) network was further analyzed using ATR-FTIR spectroscopy, providing insight into the consumption of both cyclic carbonate precursors. The formulation incorporated two distinct cyclic carbonates, each serving a specific function in the foaming process. Due to their structural differences,





**Table 1** Formulations, properties, and theoretical biobased content of PC foams

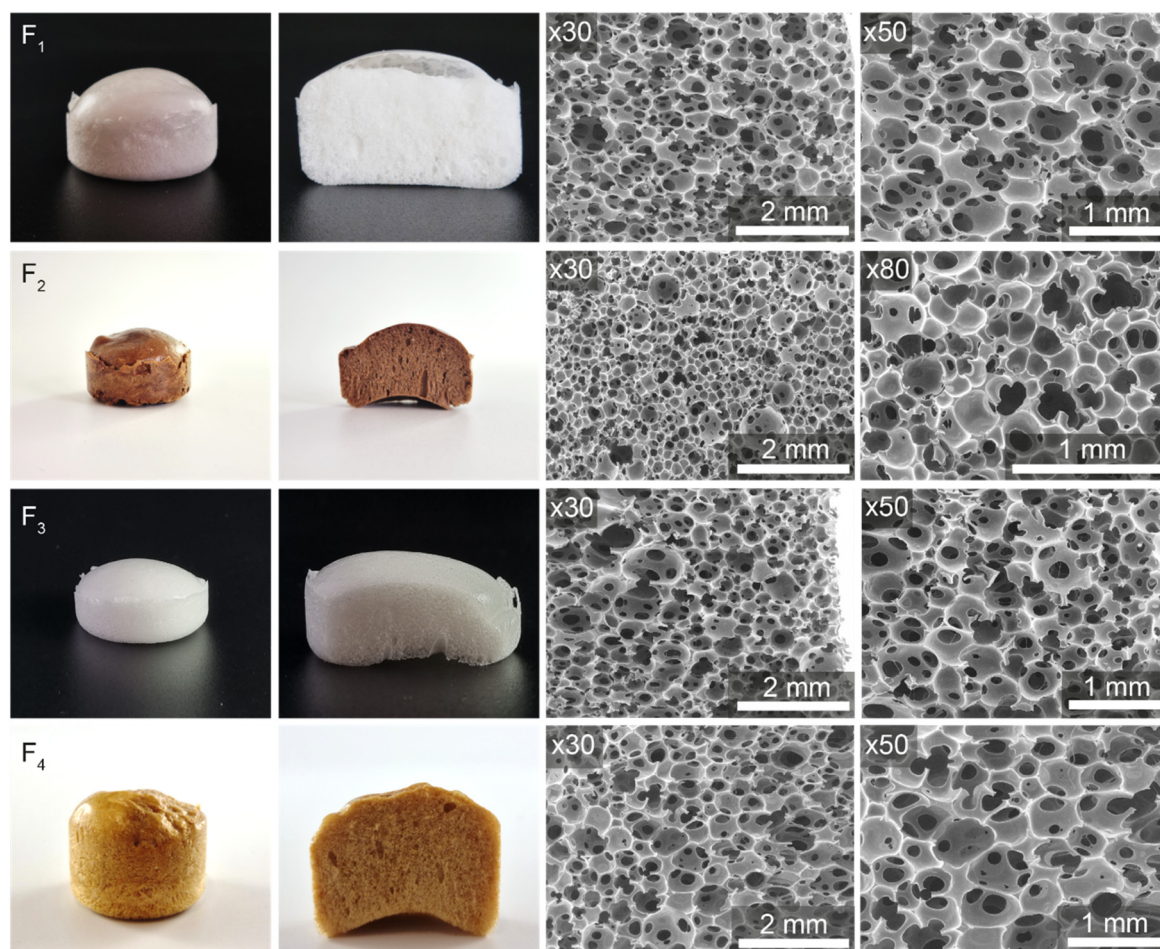
Entry	Polyol	Density [kg m <sup>-3</sup> ]	Cell size [mm]	$A_h/A_c$ <sup>a</sup> [%]	GC <sup>b</sup> [%]	$T_g$ [°C]	$T_{d5\%}$ [°C]	Biobased content [wt%]
F <sub>1</sub>	Sovermol	170 ± 2	0.52 ± 0.22	14.8	73 ± 2	−15	140	27
F <sub>2</sub>	Cardolite	174 ± 3	0.30 ± 0.09	13.2	78 ± 1	−19	170	34
F <sub>3</sub>	Priplast	356 ± 26	0.55 ± 0.23	14	67 ± 1	−55 <sup>c</sup>	175	41
F <sub>4</sub>	Lignin-PEG	113 ± 12	0.60 ± 0.17	14.5	71 ± 5	−25	150	25

<sup>a</sup>  $A_h/A_c$  represents the ratio of cell-face hole area ( $A_h$ ) to cell-face area ( $A_c$ ). <sup>b</sup> GC indicates the gel content measured after immersing for 24 h in THF. <sup>c</sup> Priplast is semi-crystalline with a melting temperature  $T_m$  of 25 °C.

these cyclic carbonates exhibit characteristic FTIR carbonyl stretching vibrations at distinct wavenumbers, differing from those of a polycarbonate network, which lacks ring strain. Spectral analysis confirms that both 5-CC and 6-CC were nearly fully consumed during polymerization, as indicated by the dominant polycarbonate carbonyl peak at  $\sim 1740$  cm<sup>-1</sup>, with only a trace residual peak for 6-CC at  $\sim 1775$  cm<sup>-1</sup>. Notably, no absorption was observed around 1800 cm<sup>-1</sup>, confirming the complete consumption of 5-CC. These results demonstrate the efficiency of the reaction in incorporating cyclic carbonate functionalities into the polymeric network (Fig. S4†).

## 2.2 Properties and morphologies of bio-based polycarbonate foams

The cellular morphology of the foams was investigated by scanning electron microscopy (SEM, Fig. 2), and their main characteristics are given in Table 1. All foams based on four different biobased polyols achieve a variety of open-cell architectures, with low to moderate densities ranging from 113 to 356 kg m<sup>-3</sup>. The use of Lignin-PEG, Cardolite, and Sovermol resulted in light weight, low-density foams with a flexible nature. In contrast, Priplast polyol produced medium-density foams, which also exhibited higher mechanical compression strength

**Fig. 2** Pictures and SEM characterization of the biobased self-blown PC foams presented in Table 1.

(Fig. 4). Notably, Cardolite used in F<sub>2</sub> resulted in the smallest cell diameter of  $0.30 \pm 0.09$  mm, whereas the other foams show larger average cell diameters between 0.52 and 0.60 mm. We reason that, in addition to its rigid aromatic cores, the increased cross-linking degree (GC = 78%) favours the formation of a foam of smaller cell size. We observe that a complex interplay of the structure and properties (hydroxyl functionality, molar mass, and viscosity) of the polyols governs the final foam properties.

Importantly, the novel biobased PC foams exhibited a high proportion of open cells, as visually confirmed by SEM (Fig. 2) and quantitatively determined by similar holes-on-cells area ratios ( $A_h/A_c$ ) ranging from 13.2 to 14.8, calculated using Fitzgerald's procedure.<sup>46</sup> These values indicate comparable open porosities. The cell-face hole area plays a crucial role in defining the open-cell structure, significantly affecting the capillary action and fluid retention. A higher  $A_h/A_c$  ratio enhances permeability, improving water absorption and diffusion, which is particularly beneficial for applications such as hydroponics.

Further insights into network formation were obtained through gel content (GC) analysis, which provided quantitative evidence of the extent of crosslinking. While the GC values of the synthesized foams may appear lower than those typically reported for PHU foams (which can reach up to 95%), this difference is attributed to the inherent reactivity of the system. Unlike amines, alcohols exhibit lower nucleophilicity, and in the case of biobased polyols, the hydroxyl groups are more sterically hindered, reducing their accessibility for reaction. Despite the challenges in determining the precise reactivity trend among polyols, the gel content was found to increase with hydroxyl functionality (Table S1†). Among the polyols tested, Cardolite, which has the highest functionality (4.1), exhibited the highest GC value, followed by Sorvenol (functionality 3), and Lignin-PEG. Priplast, which possesses the lowest OH functionality (2), yielded the lowest GC values. This trend highlights the direct influence of the polyol structure on network formation.

The thermal stability and glass transition temperature ( $T_g$ ) of the foams were determined by thermogravimetric analysis (TGA) and differential scanning calorimetry (DSC), respectively. The results are listed in Table 1 (all TGA and DSC thermograms are provided in the ESI, Fig. S5 and S6†). The degra-

dation temperatures at 5% mass loss ( $T_{d5\%}$ ) for the foam samples were between 140 and 175 °C. All four of the foams have low  $T_g$ s (approximately −55 to −15 °C). Interestingly, despite lignin's aromatic units, the Kraft lignin-based polyol with free PEG chains and a low lignin content of 25 wt% contributes to the relatively low  $T_g$  of F<sub>4</sub> (−25 °C). Similarly, the flexible alkyl side chains of cardanol that fill the space between the aromatic cores result in a low- $T_g$  flexible foam ( $T_g$  of F<sub>2</sub> is around −19 °C). This behavior was also observed for the CNSL-based PHU foams produced using the same thiol-triggered CO<sub>2</sub> blowing method.<sup>47</sup> Additionally, Priplast is semi-crystalline; therefore, F<sub>3</sub> exhibits a melting temperature close to room temperature ( $T_m$  = 25 °C). The use of biobased polyols not only augmented the sustainability of the reported foams by the use of renewable resource precursors but also permitted the expansion of thermal properties in comparison to our previous study ( $T_g \approx -15$  °C).

In the context of a proof of concept for potential hydroponic applications, open-cell structures of foams with low  $T_g$  promote structural flexibility, potentially making them more suitable for hydroponic use than closed-cell rigid foams, as they allow for fluid and air permeability, elastic resilience, and root growth and penetration. Regarding the cell size, all developed foams appear suitable for root development, as root diameters can be as small as 0.2 mm, depending on plant species and age.<sup>48</sup>

To investigate the water absorption capabilities of these foams – an essential property for delivering water and nutrients to roots – we measured their water uptake over a 72-hour period ( $w$ , see Table 2) and compared it with commercial PU foams used in hydroponics. As shown in the kinetic evolutions in Fig. 3a, all foams reach saturation in less than 24 h. F<sub>4</sub>, derived from Lignin-PEG, and F<sub>2</sub>, derived from CNSL-based Cardolite, exhibit higher water uptakes of 8.9 and 7.7 g g<sup>−1</sup>, respectively. A comparison with the literature indicates that these values are comparable to those of hydroponic PU foams.<sup>49</sup> In contrast, Priplast and Sovermol reduce the water absorption capacity by a factor of ~3 for F<sub>3</sub> and F<sub>1</sub>, respectively, most likely due to differences in the hydrophilicity of the polyol.<sup>50,51</sup>

Long-term water stability is another key factor for reusable hydroponic substrates. To assess this, the four foams were subjected to *in vitro* degradation in neutral pH water for 40 days. Fig. 3b clearly reveals minimal mass losses (as low as 13%), thus indicating the excellent water stability of our cross-linked foams.

Once confirming the appropriate swelling degree as well as the appropriate stability in an aqueous environment, we analyzed the properties of the foam by compression tests. A comparison of the compressive properties of the foams is displayed in Fig. 4a and all values are summarized in Table 2. All the stress-strain ( $\sigma$ - $\epsilon$ ) curves exhibit three regimes of deformation: (i) a nearly linear elastic regime, (ii) a relatively flat stress plateau, and (iii) an abrupt stress-increase regime, like conventional elastomeric foams.<sup>2</sup> An important feature of Priplast's semi-crystalline nature contributes to higher stiffness and strength of F<sub>3</sub> ( $E$  = 1 kPa and  $\sigma$  = 96 kPa at 60% compression).<sup>52</sup>

**Table 2** Water uptake capacity, stability in water, and mechanical properties of the biobased PC foams

Entry	$w^a$ [g g <sup>−1</sup> ]	Remaining mass <sup>b</sup> [%]	$E$ (kPa)	$\sigma^c$ [kPa]
F <sub>1</sub>	$3.3 \pm 0.1$	$88.5 \pm 0.8$	$0.24 \pm 0.04$	$23 \pm 4$
F <sub>2</sub>	$7.7 \pm 0.1$	$91.6 \pm 0.2$	$0.45 \pm 0.36$	$30 \pm 16$
F <sub>3</sub>	$3.5 \pm 0.2$	$88.8 \pm 0.2$	$1.0 \pm 0.4$	$96 \pm 18$
F <sub>4</sub>	$8.9 \pm 0.4$	$86.6 \pm 0.5$	$0.10 \pm 0.04$	$8 \pm 1$

<sup>a</sup>Equilibrium water uptake ( $w$ ) after 3 days. <sup>b</sup>Remaining mass after immersion in distilled water for 40 days. <sup>c</sup>Compressive stress at 60% of compressive strain.



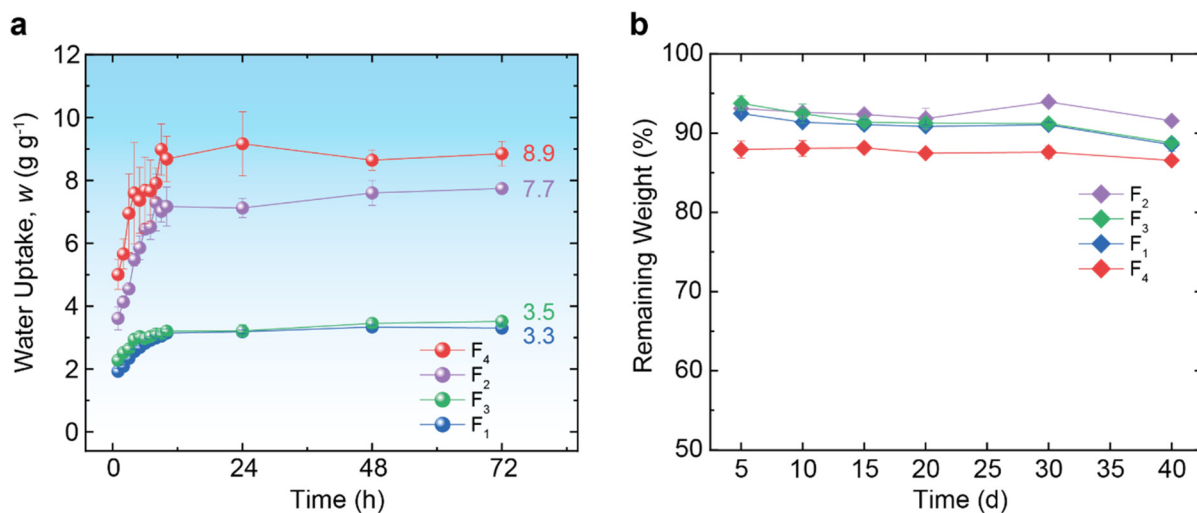


**Fig. 3** Water uptake and stability of the biobased self-blown PC foams over time. (a) Maximum ( $w = 8.9 \text{ g g}^{-1}$ ) and minimum ( $w = 3.3 \text{ g g}^{-1}$ ) water uptake within 72 h, depending on the polyols used. (b) *In vitro* degradation behavior of the foams in neutral pH water for 40 days.

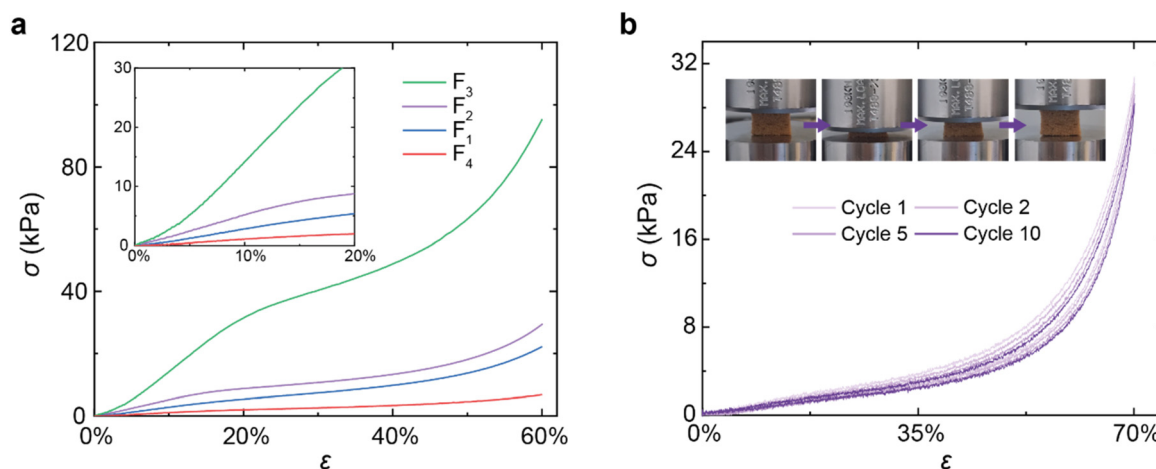


**Fig. 4** Mechanical properties via compression testing of the biobased self-blown PC foams. (a) Stress-strain ( $\sigma$ - $\epsilon$ ) curves of foams  $F_1$ - $F_4$  with different biobased polyols. (b)  $\sigma$ - $\epsilon$  curves of the CNSL-based foam,  $F_2$ , for 10 compression and release cycles up to 70% strain. Inset: photographs of  $F_2$  being subjected to cyclic compression.

Furthermore,  $F_3$ , as expected, shows a correlated increase in compressive strength with increasing foam density, whilst the low-density lignin-based  $F_4$  displays a significant loss in mechanical properties ( $E = 0.1 \text{ kPa}$  and  $\sigma = 8 \text{ kPa}$  at 60% compression). Meanwhile, the CNSL-based PC foam,  $F_2$ , combines high stiffness and strength with a high-water uptake capacity, as well as ensuring water stability.

Given these appealing features, it is feasible to use  $F_2$  as physical support for plants. We then performed a multi-cycle compression test (Fig. 4b) to assess the structural resilience of  $F_2$ . After 10 compression and release cycles at a constant strain of  $\epsilon = 70\%$ , the maximum-stress loss is only 7.8% (retention of maximum stress is 92.2%). The unloading curves almost returned to the original points, indicating that the CNSL-based foam fully recovered its original shape without plastic deformation.

The inset photographs further demonstrate the foam's ability to maintain its morphological integrity after repeated deformations. This underlines the importance of good preservation of its structural stability for successive growth cycles. Furthermore, the CNSL-based foam also maintains high resilience to repetitive deformation in the wet state (see Video S1†).

### 2.3 Exploring polycarbonate foam as a sustainable growing medium for vegetables

The biomass demand from a growing population for both food and non-food uses causes water stress and land degradation, potentially threatening food security and the environment.<sup>53–55</sup> Recently, hydroponics, aimed at mitigating land and water degradation, has become increasingly important for soilless food production in urban areas where vacant arable land is





limited.<sup>56,57</sup> In hydroponic systems, soilless growing media are intensely exploited to support seed germination and seedling growth.<sup>58–61</sup>

As a proof-of-concept application, we evaluate the suitability of the CNSL-based foam, F<sub>2</sub>, as a plant growth substrate in

soilless germination. This experiment aims not only to assess its potential as a growth medium but also to demonstrate the foam's biocompatibility with seedlings. Fig. 5a schematically illustrates the experimental setup with an LED-based white light source and the germination procedure (see Fig. S7†). Bok



**Fig. 5** Hydroponic plant growth on bio-based PC foam. (a) Schematic representation of the hydroponic setup using cashew nutshell-based foam F<sub>2</sub> as a growing medium, with regular water supplementation and a white LED light source providing a 12-hour photoperiod at 21 °C and 70–75% relative humidity. (b) Bok choy seed germination and growth monitored for 12 days. (c) Seed germination and early seedling growth of lettuce on the foam block over a period of 10 days. (d) Radish plants grown hydroponically on the same foam block used in (c), demonstrating its reusability and suitability for different plant species. (b–d) The scale bar is 2 cm.



choy (*Brassica rapa chinensis*) and lettuce (*Lactuca sativa*) were chosen as representatives of green leafy vegetable crops; radish (*Raphanus sativus*) was selected as a representative of root vegetable crops. For all three crops, seeds were sown into rectangular foam blocks in drinking water at 21 °C and 70–75% relative humidity (RH) and were investigated under daily 12:12 h light/dark cycles that simulate a full day. Bok choy sprouts visibly starting at day 4 post-sowing, with the plant's young stem gradually elongating over 12 days (Fig. 5b), or alternatively, lettuce seeds germinate successfully and develop into 10-day-old healthy seedlings (Fig. 5c). These results indicate that the foam does not exhibit toxic effects on seed germination, reinforcing its biocompatibility.

Growing different crop species on the CNSL-based foam is also possible. To further investigate the properties of CNSL-foams in the germination process, we evaluated their light transmittance as it is known that certain wavelengths can inhibit seed germination.<sup>62</sup> For this analysis, we measured the amount of light passing through ~7.5 mm thick foam samples (average position of the seed during germination) and found that only 0.26% of the light was transmitted (Fig. S9†). These results suggest that the reduced light exposure provided by the CNSL-foam creates a low-light environment similar to natural soil conditions, which may be beneficial for seed germination.

Subsequently, the same foam block used for lettuce seed germination was directly reused without further treatment for radish seeds as shown in Fig. 5d, allowing them to germinate and establish robust seedlings over a 10-day period. The roots of lettuce and radish penetrating the foam (Fig. S10,† ESI†) show that its bulk density and porosity allow for root growth and water transport. Therefore, the CNSL-based foam offers great potential for reuse in successive growth cycles owing to its ability to maintain original properties (mechanical stability, water absorption capacity).<sup>63</sup>

### 3 Conclusion

This study has shown the successful elaboration of different self-blown polycarbonate (PC) foams using a range of various renewable polyols from vegetable oils, cashew nutshell liquid, and lignin, with a combination of bis(6-CC), 5-CC, and tetra-thiol. Homogeneous foams achieving diverse open-cell structures and properties were produced from a single formulation for biobased polyols that vary in hydroxyl functionality, molar mass, and chemical structure. Importantly, we found that the cashew nutshell-based PC foam that combines high-water uptake ability and hydrolytic stability with mechanical robustness properties can serve as a viable hydroponic growing medium (solid substrate) for different vegetable species. It was furthermore shown that such foam can be directly reused for subsequent seedling growth. Additionally, incorporating biobased functionalities into self-blowing PC networks can give rise to unprecedented performance advantages. For example, the inherent antimicrobial properties of CNSL<sup>42</sup> might be useful in providing protection against plant pathogens, deser-

ving further investigation in the future. These results with successful foam-to-film recycling of the reported PC foams (Fig. S11†) motivate a closer inspection in future screening enzymatic degradation to arrive at a full understanding of the potential benefits of the foam materials. In this study, we presented the first proof-of-concept application of new biobased self-blown PC foams as a green and sustainable substrate for soilless agriculture that may be applied in urban food farming, which is increasingly relevant for future societies.

## 4 Experimental section

### 4.1 Materials

Ethylene carbonate (C<sub>5</sub>, Sigma Aldrich, 98%), pentaerythritol tetrakis(3-mercaptopropionate) (PETMP, Sigma Aldrich, >95%), and 1,8-diazabicyclo[5.4.0]undec-7-ene (DBU, Fisher Scientific, 98+%) were used as received. An epoxy-functionalized polydimethylsiloxane oligomer (TEGOMER E-Si 2330) was provided by Evonik/Quimidroga. Sovermol 750 (branched polyether/ester polyol) was supplied by BASF (Germany). Cardolite NX-9004 (novolac-type phenolic polyol) was obtained from Cardolite Specialty Chemicals. Priplast 3162 (semi-crystalline dimer fatty acid-based polyester polyol) was provided by Croda. Softwood Kraft lignin (Biopiva™ 395) was obtained from UPM. It was dried overnight in a vacuum oven at 40 °C before use. The lignin contains 2.21, 3.90 and 0.14 mmol g<sup>-1</sup> of aliphatic OH, phenolic OH and COOH, respectively, as determined by <sup>31</sup>P NMR.

### 4.2 Methods and characterization

**4.2.1. Nuclear magnetic resonance (NMR) spectroscopy.** <sup>1</sup>H NMR analyses were performed on a Bruker Avance DPX 300 spectrometer using CDCl<sub>3</sub> at ambient temperature. <sup>31</sup>P NMR was used to quantify the *hydroxyl value* (*I*<sub>OH</sub>) of the lignin-based polyol, Lignin-PEG, with a Bruker 400 MHz spectrometer. Quantitative <sup>31</sup>P NMR was performed following a similar multistep protocol as previously reported in the literature.<sup>38</sup>

A desktop scanning electron microscope (SEM, Hitachi TM3030) was used to determine the *cell size and morphology* of the PC foams. Based on the SEM images, the cell size distributions were calculated by averaging the diameter measurements of at least 100 cells. The areas of cell faces (*A*<sub>c</sub>) and holes (*A*<sub>h</sub>) were estimated using ImageJ software. For each sample, the areas of 20 cells and their corresponding cell hole areas (if present) were measured with the elliptical selection tool. The holes-on-cells area ratio *A*<sub>h</sub>/*A*<sub>c</sub> was then calculated for each cell and averaged to get the final value. Only holes with clearly visible dark pixels were considered.

**4.2.2. Foam density.** Foam density was evaluated in triplicate by weighing foam and dividing it by its volume, with volumes of around 1 cm<sup>3</sup>.

**4.2.3. Gel content (GC).** Three samples were weighed (*m*<sub>1</sub>) before being immersed in tetrahydrofuran for 24 h. Afterward, tetrahydrofuran was removed, and the samples were dried at





room temperature for at least 48 h, followed by drying under vacuum for 24 h ( $m_2$ ). The gel content ( $G$ ) was calculated using the formula:  $G = 100 \times \frac{m_2}{m_1}$ .

Glass transition temperatures of the foams were measured using a *differential scanning calorimeter* (DSC 25, TA Instruments). The samples were analyzed at a heating rate of  $10\text{ }^\circ\text{C min}^{-1}$  over a temperature range from  $-80$  to  $80\text{ }^\circ\text{C}$  under a  $\text{N}_2$  atmosphere. The glass transition temperature ( $T_g$ ) values were obtained from the second heating scan.

**4.2.4. Thermogravimetric analysis.** Thermogravimetric analysis (TGA) was performed using a TGA Q500 from TA Instruments. Around 5 mg of samples were heated from  $40$  to  $800\text{ }^\circ\text{C}$  at a rate of  $10\text{ }^\circ\text{C min}^{-1}$  under a  $\text{N}_2$  flow.

**4.4.5. Rheological measurements.** Time sweeps were conducted at 1% strain and 1 Hz at  $70\text{ }^\circ\text{C}$  using an ARES rheometer (Rheometrics).

**4.4.6. Compression tests.** Compression tests were performed on an Instron 5569 universal testing machine with a 5 kN load cell. Compression was performed at a rate of  $1\text{ mm min}^{-1}$  on cubic foam samples of about  $1\text{ cm}^3$ . Young's modulus was calculated from the slope at the beginning (*i.e.* 1–4 strain %) of the stress–strain curve. At least three samples were tested to calculate the strength and modulus. The cyclic compression tests at 70% strain were conducted at the rate of  $10\text{ mm min}^{-1}$ .

**4.4.7. Attenuated total reflection (ATR)-FT-IR spectra.** Attenuated total reflection (ATR)-FT-IR spectra were recorded using a ThermoFisher Nicolet iS20 spectrometer equipped with a diamond crystal-based ATR accessory. Spectra were obtained with 32 scans at a resolution of  $4\text{ cm}^{-1}$  in the range of  $4000$ – $500\text{ cm}^{-1}$ .

### 4.3 Synthesis procedure

**4.3.1 Synthesis of the lignin-based polyol (Lignin-PEG).** Kraft lignin and polyethylene glycol (PEG,  $M_n = 300\text{ g mol}^{-1}$ ) were introduced into a 250 mL three-neck flask to prepare 50 g of a Lignin-PEG mixture, with a lignin content of 25 wt%. After mechanical stirring, ethylene carbonate (2 molar equivalents with respect to the number of lignin hydroxyl groups) and  $\text{K}_2\text{CO}_3$  (0.1 molar equivalent of ethylene carbonate) were added to the mixture. The reactor was then placed under an argon flow and immersed in an oil bath at  $110\text{ }^\circ\text{C}$ . The reaction took place for 4 h. A homogeneous liquid polyol was obtained, and no further purification was needed.

**4.3.2 Synthesis of di(trimethylolpropane) carbonate ( $\text{BC}_6$ ).** Di(trimethylolpropane) (52.0 g, 208 mmol, 1 eq.), triethylamine (126.1 g, 1246 mmol, 6 eq.), and 630 mL anhydrous THF were added to a 2-neck round-bottom flask. The solution was then cooled in an ice bath. While stirring, ethyl chloroformate (130.7 g, 1205 mmol, 5.8 eq.) in 200 mL anhydrous THF was added dropwise from a dropping funnel under a nitrogen atmosphere, and a white precipitate formed. The reaction mixture was allowed to warm to room temperature and stirred overnight. The white precipitate was filtered off, and the solvent was removed using a rotary evaporator.  $\text{BC}_6$  was recrystallized 3 times from diethyl ether and isolated as a white solid

(25.1 g, 40%).  $^1\text{H NMR}$  (300 MHz,  $\text{CDCl}_3$ ):  $\delta$  4.29 (d,  $J = 10.1\text{ Hz}$ , 4H,  $-\text{CH}_2\text{OCOOCH}_2-$ ), 4.17 (d,  $J = 10.5\text{ Hz}$ , 4H,  $-\text{CH}_2\text{COOCH}_2$ ), 3.50 (s, 4H,  $-\text{CH}_2\text{OCH}_2-$ ), 1.50 (q,  $J = 7.5\text{ Hz}$ , 4H,  $-\text{CH}_3\text{CH}_2\text{C}-$ ), 0.91 (t,  $J = 7.6\text{ Hz}$ , 6H,  $\text{CH}_3\text{CH}_2\text{C}-$ ). The  $^1\text{H NMR}$  spectrum matches the previously published data.<sup>64</sup>

### 4.3.3 Procedure for the preparation of biobased self-blown PC foams

*Representative procedure described for  $\text{F}_2$ .* To a 25 mL PTFE beaker charged with PETMP (0.808 g, 1.654 mmol), Cardolite (1.0 g, 0.807 mmol), and TEGOMER E-Si 2330 (0.258 g) was added  $\text{BC}_6$  (2.0 g, 6.616 mmol) and  $\text{C}_5$  (0.583 g, 6.616 mmol). The mixture was heated to  $70\text{ }^\circ\text{C}$  to ensure complete melting of all the reactants, and then DBU (0.063 mL, 0.413 mmol, 3.13 mol% with respect to the cyclic carbonates) was added to this mixture. After mechanical mixing for 10 minutes, the reactive formulation was cured in an oven for 1 h at  $70\text{ }^\circ\text{C}$ . Note that for  $\text{F}_1$  and  $\text{F}_3$ , the DBU content was increased to 5 mol%.

### 4.4 Water uptake and water stability tests

To calculate the *water uptake* ( $w$ ), the measured sample weights at various times after immersion in distilled water were divided by the initial dry weight of the sample before immersion.

For each type of foam, three samples ( $3 \times 6 = 18$  total) were immersed in distilled water to evaluate *water stability* over a 40-day period. For example, at specific intervals, such as after 5 days, three samples were taken out and dried in a vacuum oven at room temperature for 72 h, and their remaining weight was measured and averaged.

### 4.5 Germination experiment

Foam blocks were placed in trays with a shallow layer of drinking water, and seeds were directly planted into the foam blocks. 10 seeds were germinated per plant type. The trays were kept in a plastic greenhouse set at  $21\text{ }^\circ\text{C}$  with 70–75% relative humidity. The seeds were then exposed to a 12-hour light (using white LEDs (6000 K) combined with red LEDs (620–660 nm) from Solight™) and 12-hour dark cycle each day, without the addition of any nutrients. The regularly watered foams were monitored for 10 or 12 days. Prior to the test, these foam blocks were washed with a 7/3 isopropyl alcohol/water solution to remove and recover any residual monomers and catalyst that could potentially contribute to toxicity.

### 4.6 Foam-to-film recycling

Foam  $\text{F}_2$  was cut into small pieces, placed between two Teflon-covered metallic plates and reprocessed *via* compression using a preheated Atlas Heated Platens from Specac. The sample was then pressed for 20 min at  $90\text{ }^\circ\text{C}$  under a pressure of 3 bar.

### 4.7 Foam light transmittance

The transmittance of incident light of the reported foams was measured using an in-house built light detector composed of a photodiode (Si PIN Photodiode BPX65 by OSRAM, wavelength sensitivity range 350–1100 nm) connected to an Arduino board to read the transmitted light intensity. Samples (average thickness of 7.5 mm) were placed at 15 cm from the LED lamps.



#### 4.8 Biobased content

The theoretical biobased content (wt%) is calculated by dividing the total mass of the biobased polyol and ethylene carbonate (sourced from CO<sub>2</sub>) by the total mass of all components in the system and then multiplying the result by 100.

### Author contributions

HS conceived the project. TA designed and conducted the experiments and was involved in the project conceptualization. PCH, AD, and LA conducted experiments for synthesizing and characterizing the lignin-based polyol. GP performed a preliminary test on hydrolytic stability. DM provided the initial hydroponic setup, which was later adapted. TA analyzed the data and wrote the manuscript. XLP and HS reviewed and edited the manuscript. LI assisted in discussing some of the results. AG conducted the TGA experiments. HS supervised the project. All authors commented on the manuscript.

### Data availability

The data that support the findings of this study are available from the corresponding author H. S. upon reasonable request.

### Conflicts of interest

There are no conflicts to declare.

### Acknowledgements

This project received funding from the European Union's Horizon 2020 research and innovation program under the Marie Skłodowska-Curie Grant Agreement No 860911. Itziar Otaegi Tena is thanked for her help with the mechanical testing.

### References

- 1 L. J. Gibson, *MRS Bull.*, 2003, **28**, 270–274.
- 2 L. J. Gibson and M. F. Ashby, *Cellular solids: structure and properties*, Cambridge University Press, Cambridge, 2nd edn, 1997.
- 3 G. C. Dsouza, H. Ng, P. Charpentier and C. C. Xu, *ChemBioEng Rev.*, 2024, **11**, 7–38.
- 4 M. Tomin and Á. Kmetty, *J. Appl. Polym. Sci.*, 2022, **139**, 51714.
- 5 F. Monie, T. Vidil, B. Grignard, H. Cramail and C. Detrembleur, *Mater. Sci. Eng., R*, 2021, **145**, 100628.
- 6 Y. Deng, R. Dewil, L. Appels, R. Ansart, J. Baeyens and Q. Kang, *J. Environ. Manage.*, 2021, **278**, 111527.
- 7 T. A. Phung Hai, M. Tessman, N. Neelakantan, A. A. Samoylov, Y. Ito, B. S. Rajput, N. Pourahmady and M. D. Burkart, *Biomacromolecules*, 2021, **22**, 1770–1794.
- 8 Official Journal of the European Union, L252, 4 August 2020, <https://eur-lex.europa.eu/legal-content/EN/TXT/PDF/?uri=OJ:L:2020:252:FULL&from=EN>.
- 9 C. Amezcua-Arranz, M. Santiago-Calvo and M.-Á. Rodríguez-Pérez, *Eur. Polym. J.*, 2023, **197**, 112366.
- 10 T. Dong, E. Dheressa, M. Wiatrowski, A. P. Pereira, A. Zeller, L. M. L. Laurens and P. T. Pienkos, *ACS Sustainable Chem. Eng.*, 2021, **9**, 12858–12869.
- 11 G. Coste, C. Negrell and S. Caillol, *Eur. Polym. J.*, 2020, **140**, 110029.
- 12 B. Grignard, J.-M. Thomassin, S. Gennen, L. Poussard, L. Bonnaud, J.-M. Raquez, P. Dubois, M.-P. Tran, C. B. Park, C. Jerome and C. Detrembleur, *Green Chem.*, 2016, **18**, 2206–2215.
- 13 H. Blattmann, M. Lauth and R. Mülhaupt, *Macromol. Mater. Eng.*, 2016, **301**, 944–952.
- 14 A. Cornille, C. Guillet, S. Benyahya, C. Negrell, B. Boutevin and S. Caillol, *Eur. Polym. J.*, 2016, **84**, 873–888.
- 15 A. Cornille, S. Dworakowska, D. Bogdal, B. Boutevin and S. Caillol, *Eur. Polym. J.*, 2015, **66**, 129–138.
- 16 F. Monie, B. Grignard and C. Detrembleur, *ACS Macro Lett.*, 2022, **11**, 236–242.
- 17 M. Bourguignon, B. Grignard and C. Detrembleur, *Angew. Chem., Int. Ed.*, 2022, **61**, e202213422.
- 18 F. Monie, B. Grignard, J. Thomassin, R. Mereau, T. Tassaing, C. Jerome and C. Detrembleur, *Angew. Chem.*, 2020, **132**, 17181–17189.
- 19 P. Wei, G. A. Bhat and D. J. Darensbourg, *Angew. Chem., Int. Ed.*, 2023, **62**, e202307507.
- 20 H. Wang, F. Xu, Z. Zhang, M. Feng, M. Jiang and S. Zhang, *RSC Sustainability*, 2023, **1**, 2162–2179.
- 21 R. M. Cywar, N. A. Rorrer, C. B. Hoyt, G. T. Beckham and E. Y.-X. Chen, *Nat. Rev. Mater.*, 2021, **7**, 83–103.
- 22 W. Yu, E. Maynard, V. Chiaradia, M. C. Arno and A. P. Dove, *Chem. Rev.*, 2021, **121**, 10865–10907.
- 23 K. Saito, C. Jehanno, L. Meabe, J. L. Olmedo-Martínez, D. Mecerreyes, K. Fukushima and H. Sardon, *J. Mater. Chem. A*, 2020, **8**, 13921–13926.
- 24 P. Durand, A. Brège, G. Chollet, E. Grau and H. Cramail, *ACS Macro Lett.*, 2018, **7**, 250–254.
- 25 N. Weingart, D. Raps, J. Kuhnigk, A. Klein and V. Altstädt, *Polymers*, 2020, **12**, 2314.
- 26 D. Jahani, A. Ameli, M. Saniei, W. Ding, C. B. Park and H. E. Nagueib, *Macromol. Mater. Eng.*, 2015, **300**, 48–56.
- 27 J. W. S. Lee, K. Wang and C. B. Park, *Ind. Eng. Chem. Res.*, 2005, **44**, 92–99.
- 28 R. Gendron and L. E. Daigneault, *Polym. Eng. Sci.*, 2003, **43**, 1361–1377.
- 29 V. Kumar and J. Weller, *J. Eng. Ind.*, 1994, **116**, 413–420.
- 30 T. Abbasoglu, D. Ciardi, F. Tournilhac, L. Irusta and H. Sardon, *Angew. Chem., Int. Ed.*, 2023, **62**, e202308339.
- 31 D. Trojanowska, F. Monie, G. Perotto, A. Athanassiou, B. Grignard, E. Grau, T. Vidil, H. Cramail and C. Detrembleur, *Green Chem.*, 2024, **26**, 8383–8394.
- 32 C. Carré, Y. Ecochard, S. Caillol and L. Avérous, *ChemSusChem*, 2019, **12**, 3410–3430.



- 33 V. Froidevaux, C. Negrell, S. Caillol, J.-P. Pascault and B. Boutevin, *Chem. Rev.*, 2016, **116**, 14181–14224.
- 34 H. Sardon, D. Mecerreyes, A. Basterretxea, L. Avérous and C. Jehanno, *ACS Sustainable Chem. Eng.*, 2021, **9**, 10664–10677.
- 35 D. Kyriacos, *Biobased Polyols for Industrial Polymers*, Wiley, 1st edn, 2020.
- 36 X. Ma, J. Chen, J. Zhu and N. Yan, *Macromol. Rapid Commun.*, 2021, **42**, 2000492.
- 37 J. Peyrton and L. Avérous, *Mater. Sci. Eng., R*, 2021, **145**, 100608.
- 38 P. Furtwengler and L. Avérous, *Polym. Chem.*, 2018, **9**, 4258–4287.
- 39 T. J. Gutiérrez, L. A. Toro-Márquez, D. Merino and J. R. Mendieta, *Food Hydrocolloids*, 2019, **89**, 283–293.
- 40 G. C. Dsouza, H. Li, Z. Yuan, C. C. Xu, M. B. Ray and A. Prakash, *J. Appl. Polym. Sci.*, 2024, **141**, e54877.
- 41 L. Pilato, *Phenolic Resins: A Century of Progress*, Springer Berlin Heidelberg, New York, 2010, pp 189–193.
- 42 C. Voirin, S. Caillol, N. V. Sadavarte, B. V. Tawade, B. Boutevin and P. P. Wadgaonkar, *Polym. Chem.*, 2014, **5**, 3142–3162.
- 43 A. Duval, D. Vidal, A. Sarbu, W. René and L. Avérous, *Mater. Today Chem.*, 2022, **24**, 100793.
- 44 Solutions from the Nature – Sovermol®, <https://www.basf.com/us/en/products/General-Business-Topics/dispersions/Products/sovermol> (accessed Jul 27, 2024).
- 45 Priplast | Smart Materials, <https://www.crodasmartmaterials.com/en-gb/product-finder> (accessed Jul 27, 2024).
- 46 C. Fitzgerald, I. Lyn and N. J. Mills, *J. Cell. Plast.*, 2004, **40**, 89–110.
- 47 N. S. Purwanto, Y. Chen and J. M. Torkelson, *ACS Appl. Polym. Mater.*, 2023, **5**, 6651–6661.
- 48 Y. Liu, G. Wang, K. Yu, P. Li, L. Xiao and G. Liu, *Sci. Rep.*, 2018, **8**, 2960.
- 49 H. Li, Z. Ali, Z. Yuan, Y. Hu, Q. Wei and C. C. Xu, *Biofuels, Bioprod. Biorefin.*, 2023, **17**, 549–563.
- 50 N. Sienkiewicz, S. Czlonka, A. Kairyte and S. Vaitkus, *Polym. Test.*, 2019, **79**, 106046.
- 51 A. Kairyte and S. Vėjelis, *Ind. Crops Prod.*, 2015, **66**, 210–215.
- 52 M. A. Sawpan, *J. Polym. Res.*, 2018, **25**, 184.
- 53 F. Zabel, R. Delzeit, J. M. Schneider, R. Seppelt, W. Mauser and T. Václavík, *Nat. Commun.*, 2019, **10**, 2844.
- 54 S. Pfister, P. Bayer, A. Koehler and S. Hellweg, *Environ. Sci. Technol.*, 2011, **45**, 5761–5768.
- 55 J. A. Foley, R. DeFries, G. P. Asner, C. Barford, G. Bonan, S. R. Carpenter, F. S. Chapin, M. T. Coe, G. C. Daily, H. K. Gibbs, J. H. Helkowski, T. Holloway, E. A. Howard, C. J. Kucharik, C. Monfreda, J. A. Patz, I. C. Prentice, N. Ramankutty and P. K. Snyder, *Science*, 2005, **309**, 570–574.
- 56 L. Xi, M. Zhang, L. Zhang, T. T. S. Lew and Y. M. Lam, *Adv. Mater.*, 2022, **34**, 2105009.
- 57 S. Ragaveena, A. Shirley Edward and U. Surendran, *Rev. Environ. Sci. Bio/Technol.*, 2021, **20**, 887–913.
- 58 A. Fussy and J. Papenbrock, *Plants*, 2022, **11**, 1153.
- 59 N. Gruda, *Agronomy*, 2019, **9**, 298.
- 60 G. E. Barrett, P. D. Alexander, J. S. Robinson and N. C. Bragg, *Sci. Hortic.*, 2016, **212**, 220–234.
- 61 M. Raviv, J. H. Lieth and A. Bar-Tal, *Soilless culture: theory and practice*, Academic press, London, 2nd edn, 2019.
- 62 Y. Wei, S. Wang and D. Yu, *Plants*, 2023, **12**, 2746.
- 63 J. M. Kovačič, T. Ciringer, J. Ambrožič-Dolinšek and S. Kovačič, *Biomacromolecules*, 2022, **23**, 3452–3457.
- 64 R. L. Snyder, D. J. Fortman, G. X. De Hoe, M. Hillmyer and W. R. Dichtel, *Macromolecules*, 2018, **51**, 389–397.

